



Design and Efficient Analysis of Large Reflectarray Antenna

I. Aryanian¹, A. Abdipour^{2*} and Gh. Moradi³

1- PhD. Student, Department of Electrical Engineering, Amirkabir University of Technology, Tehran, Iran

2- Professor, Department of Electrical Engineering, Amirkabir University of Technology, Tehran, Iran

3- Associate Professor, Department of Electrical Engineering, Amirkabir University of Technology, Tehran, Iran

ABSTRACT

In recent years reflectarray antennas have received considerable attention due to their unique capabilities. However, due to their large size, analyzing the performance of these antennas using traditional full wave finite-difference and finite-element techniques requires considerable computational resources. In this paper, we present an efficient method to accurately analyze these class of antennas which considerably reduces the computational burden. First, the radiation properties of the unit cells of the antennas are obtained by applying periodic boundary conditions, which corresponds to an infinite array. Then, a phase-only algorithm is used to obtain required phase shift on the antenna surface. Next, different unit cells are used to achieve the required phase on the antenna surface. Lastly, to confirm the validity of our approach, each designed antenna is simulated by full wave method using method of moment and the full wave simulation results of co and cross polarization levels are compared with those obtained using the proposed formula. There is excellent agreement between the co- and cross polarization levels obtained by proposed approach and those obtained using full wave simulation.

KEYWORDS

Full Wave Simulation, High Gain Antenna, Reflectarray Antenna, Unit Cell Diversity.

*

Corresponding Author, Email: abdipour@aut.ac.ir

1- INTRODUCTION

The planar reflectarray combines the advantages of conventional parabolic reflectors and phased array antennas. It provides some attractive features such as low mass and small volume. Also, as reflectarray can be implemented on a flat panel, without the need for molds like reflector antennas, manufacturing process is easier. Another advantage of reflectarray antenna is its capability to use active elements, which enables one to control the radiation pattern of the antenna. A microstrip reflectarray antenna is a low profile planar reflector that consists of microstrip patch arrays printed on a dielectric substrate. Antenna surface is illuminated by a feed antenna which imposes amplitude of electric field on the array. Individual elements of the array are designed to generate required reflection phase shift so that the reflected energy from the array is collimated to form a main beam in a given direction or to generate a shaped beam in the coverage area. There are several methods to tune the phase shift in each cell such as varying the size of the resonating patches, [1-2] using a transmission line of proper length, or aperture-coupled to the patches [3-6]. Additionally, the phase can be controlled by adding active elements to the antenna [7-8]. Different methods can be used to add reconfigurability to the reflectarray antenna, using microstrip elements with an integrated electronic control, like MEMs-based structures [9], varactor loaded patches [10,11], PIN diodes [12-18] or liquid crystal based structures [19]. The antenna beam can be switched to different angles using PIN diode. Another method is using ring elements with variable size like square ring, circular ring, dual square rings, dual circular rings [20], multi cross loop [21], and combination of cross and rectangle loop elements [22].

In this paper, a few unit cells provide the best phase response, are chosen to be studied and a comparison between their performances is performed to give a good view of different unit cell shapes response. We also introduce a design procedure based on array theory and derive analytical expressions to estimate co- and cross polarization levels. To synthesize the radiation pattern in the frequency band from 11 GHz up to 11.7 GHz, a phase-only synthesis technique is used and the amplitude distribution is imposed by the feed and required phase shift on the antenna surface is evaluated. Next, different unit cell geometries are designed and simulated using full wave simulation software (HFSS). These cells are used to impose the required phase on the antenna surface. Finally to confirm our derivations, we compare our results with those obtained using full wave simulations. Here it is important to emphasize that the traditional full wave analysis of reflectarray antennas is computationally very expensive and not practical for large antennas, whereas our method considerably reduces the computational burden while generating accurate results.

2- REFLECTARRAY DESIGN

The first step to design a reflectarray antenna is to select an appropriate element with enough phase range. After designing the element, antenna can be designed in a four step process. First, size of the antenna should be estimated using desired gain by:

$$G = \eta \frac{4\pi A}{\lambda^2} \quad (1)$$

where G is the antenna gain, η is the efficiency, A is the area of the antenna, and λ is the free space wave length. The feed location is calculated to have the maximum efficiency. Next, electric field on the array surface is determined, and lastly, compensating phase of each element is determined to obtain desired pattern. After these four steps and choosing the length of each element, the antenna is designed and overall pattern can be obtained.

A. ELEMENTS DESIGN

In this part a few unit cell structures with different geometries are simulated using HFSS software to obtain their phase response. This simulation assumes infinite array which gives a good approximation of the reflected phase from the element using Floquet modes [23]. To obtain the radiation properties of an infinite array, we apply periodic boundary conditions to each unit cell. The geometries of different unit cells which we consider for our reflectarray antennas are shown in Fig. 1 and the corresponding dimensions are given in Table 1. Element length in Fig. 1 is a parameter of the unit cells, which varies to produce different phase responses. Element length in Fig.1 (a) is the patch length, designated by L . Also, in Fig. 1(b), 1(c) and 1(d) the loop length L and in Fig. 1(e) and 1(f) the stub length connected to the circular patch L and Fig. 1(g) is the bottom layer patch length L_1 are used to vary the phase response. Designed unit cells are rectangular patch [1], double square ring [20], rectangle and cross ring [21], double cross ring [23], three layer rectangular patch [24], circular patch with one stub [25], and circular patch with two stubs [26]. Rectangular patch, double square ring, rectangle and cross ring, double cross ring, and three layer rectangular patch are dual polarized and have the same response to the waves with orthogonal polarization but circular patch with one stub, and circular patch with two-stub elements are single polarized cells which make phase change to the waves which are parallel to the line connecting the stub to the patch. Phase of simulated reflected wave against element length at 11 GHz for different unit cells is shown in Fig. 2 and Fig. 3 and as an example of phase response in the frequency band; phase response of double cross ring element is shown in Fig. 4.

Fig. 3 shows that rectangular patch produce a phase shift of about 300 degrees which is not good enough for designing a reflectarray antenna. Moreover, double square ring, rectangle and cross ring and double cross loop produce a phase shift of about 600 degrees and three layer patch has a phase variation of about 400 degrees.

Moreover, Fig. 2 shows that circular patch with one stub can produce a phase shift of about 900 degrees and circular patch with two stubs can produce a phase shift of about 600 degrees.

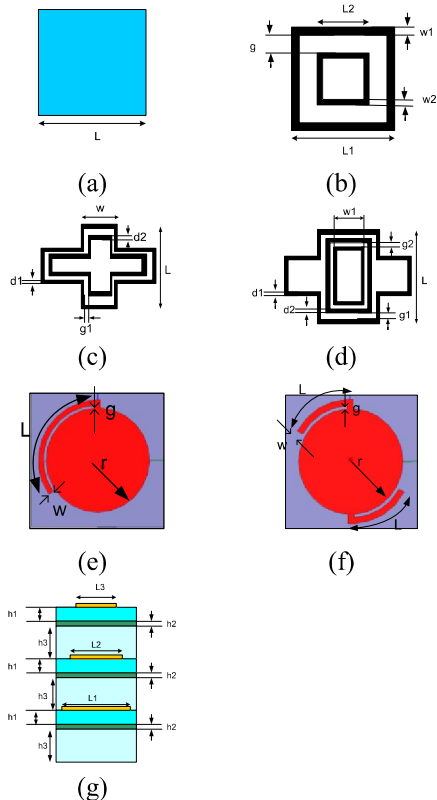


Fig. 1. Different shape cells, (a) rectangular patch, (b) double square ring, (c) double cross ring, (d) rectangle and cross ring, (e) circular patch with one stub, (f) circular patch with two stubs, (g) three layer rectangular patch

TABLE 1. UNIT CELL PARAMETERS

UNIT CELL SHAPE	CELL PARAMETER (mm)	DIELECTRIC CONSTANT OF SUBSTRATE	HEIGHT OF SUBSTRATE (mm)	CELL SIZE (mm)
RECTANGULAR PATCH	L	2.2	1.6	14
DOUBLE SQUARE RING	$w1=.6, w2=.6, g=.5$	2.17	3.175	12
DOUBLE CROSS RING	$d1=.3, d2=.3, g1=.5, w=2.8$	2.17	3.175	12
RECTANGLE AND CROSS RING	$d1=.3, d2=.3, d3=.3, g1=.6, g2=.3, w1=1$	2.17 1.067	0.144 3.03	12
CIRCULAR PATCH WITH ONE STUB	$r=3.9, g=0.2, w=0.384$	3.38	0.81	10
CIRCULAR PATCH WITH TWO STUBS	$r=3.27, g=0.2, w=0.384$	3.38	0.81	8.6
THREE LAYER RECTANGULAR PATCH	$h1=0.144, h2=0.05, h3=3, L2=0.9 \times L1, L3=0.7 \times L1$	2.7 2.2 1.06	0.05 0.144 3	14

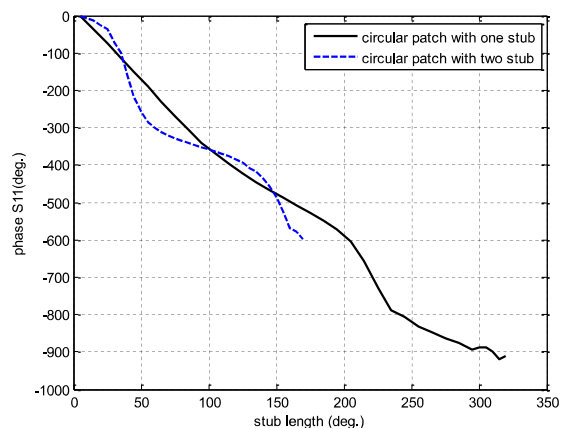


Fig. 2. Phase of simulated reflected wave against element length at 11 GHz for circular patch with one or two stubs

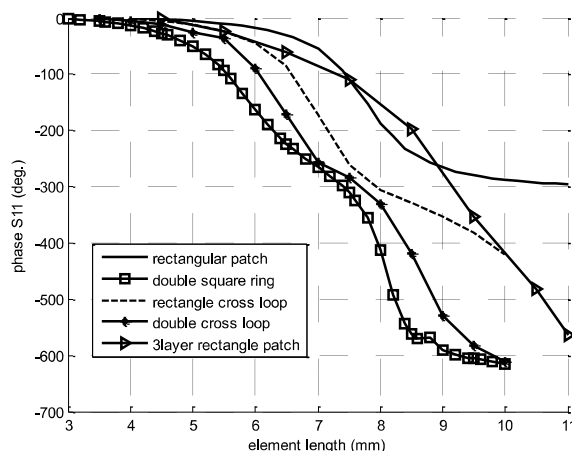


Fig. 3. Phase of simulated reflected wave against element length at 11 GHz for different shape cells

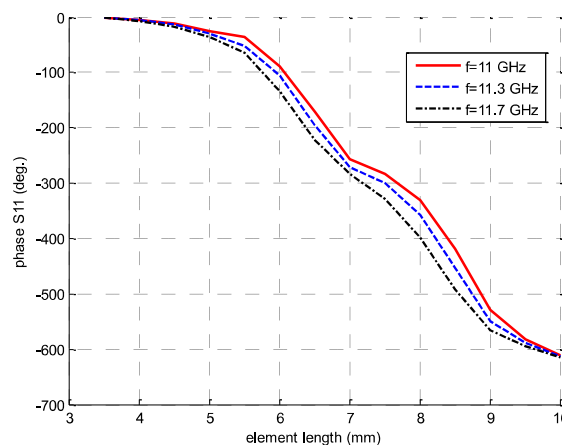


Fig. 4. Phase of simulated reflected wave against element length at 11 GHz, 11.3 GHz, and 11.7 GHz for double cross ring

B. ANTENNA DESIGN

Antenna surface is rectangular, and size of the antenna is determined by (1). For a gain of about 27 dB, $\eta = 0.7$ and at 11 GHz, required area of the antenna is 0.0424 m^2 . Length of the antenna is determined from the square root of its area that is 0.2059 m. The number of the elements of the antenna is simply obtained by dividing the area of the

antenna to the area of a unit cell. To avoid the appearance of grating lobes, elements are linearly spaced with about half a free space wavelength in both directions. Antenna size, focal length, unit cell size, and number of elements of different designed antennas are shown in Table 2.

The focal length of the antenna is designed to have maximum efficiency. Therefore, efficiency for different feed locations is calculated and then the best one is selected.

TABLE 2. DESIGN PARAMETERS FOR DIFFERENT ANTENNAS

UNIT CELL SHAPE	CELL SIZE (MM)	NUMBER OF CELLS	FOCAL LENGTH (CM)
RECTANGULAR PATCH	14	15×15	26
DOUBLE SQUARE RING	12	17×17	25
DOUBLE CROSS RING	12	17×17	25
RECTANGLE AND CROSS RING	12	17×17	25
Circular patch with one stub	10	21×21	26
Circular patch with two stubs	8.6	23×23	25
Three layer rectangular patch	14	17×17	30

Next, each element's position is computed and phase of the feed is determined in these locations by calculating the distance from the feed. Phase of the center element is considered to be zero and other elements phase is computed from the center element.

C. PHASE COMPENSATION

For our analysis, we assume monochromatic waves with $e^{j\omega t}$ time-variation. The compensating phase of each element should be determined to have a focused beam in the desired direction. We consider an antenna consisting of N reflecting elements that are illuminated by a feed located at the focal point of the antenna. Assuming a horn feed illuminating the individual patches, the excitation terms are proportional to the magnitude and phase of the electric field at the n^{th} patch. The amplitude variations between elements is negligible and thus we only consider the phase variations. Hence, the main factor that affects the reflected field from each cell is the distance between the feed phase center and the n^{th} element phase center (R_n). Also, the feed has a certain angular taper over the antenna surface which can be included in the pattern analysis by multiplying the relative complex excitation term by a raised cosine factor [8] that can be adjusted to match the pattern of the actual feed by choosing the proper q .

Feed antenna is modeled by its radiation pattern both in our approach and the full wave simulation. The angular

taper of the feed can be modeled as $\frac{e^{-jkR_n}}{R_n} \cos \theta_n^q$, where q

is the exponent of the feed pattern function represented by $\cos^q \theta$. The quantity q is determined from the taper factor at the edges of the reflectarray, which is about -10 dB for a focused beam 0 and therefore, q is calculated to be 13. Consequently, by multiplying the complex excitation term by the compensating phase factor $e^{-jk\psi_n}$ resulted from each element, the complex reflected field from each element can be expressed in the form

$$\frac{\cos \theta_n^q}{|R_n|} e^{-j(kR_n - \psi_n)} \quad (2)$$

in which ψ_n is the compensation phase of the n^{th} element. In order to convert the spherical wave radiated by the horn into a focused beam, the field must be reflected from each element with an appropriate phase shift. This phase shift is adjusted independently for each element to produce a progressive phase distribution of the reflected field on the planar surface that generates a pencil beam in a given direction, as is known from classic phased array theory. So, the required phase shift at each element to produce a collimated beam in a given direction is [6]:

$$\psi_n = k_0 (R_n - (x_n \cos \phi_b + y_n \sin \phi_b) \sin \theta_b) \quad (3)$$

where θ_b, ϕ_b shows the beam direction, k_0 is the free space wavenumber, and (x_n, y_n) is the coordinates of element n . Accordingly, by considering the curve of the phase change by element length change, the length of each element can be determined. To have a wideband antenna the achieved phase should be optimized in the required frequency band. Thus, a cost function is used to reduce the error in the frequency band which is:

$$e(n) = \sum_{f_i=l,c,u} |\Phi^{\text{desired}}(f_i)(n) - \Phi^{\text{achieved}}(f_i)(n)| \quad (4)$$

where $\Phi^{\text{desired}}(f_i)(n)$ is the desired phase in the location of element n obtained by (3) in the lower, centre, and upper frequency of the frequency band and $\Phi^{\text{achieved}}(f_i)(n)$ is the achieved phase. This cost function compares the phase obtained from the element and desired phase and chooses the best element length which reduces the cost function.

3- ANTENNA ANALYSIS

After choosing size of the elements, antenna gain can be calculated using the input power to the feed horn P_F , according to [22] as:

$$G(\theta, \varphi) = \frac{4\pi r^2}{2\eta_0 P_F} |E(\theta, \varphi)|^2 \quad (5)$$

where η_0 is the intrinsic impedance of free space, $|E(\theta, \phi)|$ is the amplitude of the far electric field, and the input power of the feed horn is [22]:

$$P_f = \frac{\pi}{\eta_0 \lambda^2 (2q+1)} \quad (6)$$

Total radiated far field is calculated from electric field of feed antenna which is:

$$E^{Fy}(\theta, \phi) = \frac{jke^{-jkr}}{2\pi r} (\hat{\theta} \cos^q \theta \cos \phi + \hat{\phi} \cos^q \theta \sin \phi) \quad (7)$$

Equation (7) gives the field radiated by the feed in spherical coordinates (r, θ, ϕ) referred to the feed coordinate system (F). Therefore, the Cartesian electric field of the feed can be expressed as:

$$\begin{pmatrix} E_x^F \\ E_y^F \\ E_z^F \end{pmatrix} = \begin{pmatrix} \sin \theta \cos \phi & \cos \theta \cos \phi & -\sin \phi \\ \sin \theta \sin \phi & \cos \theta \sin \phi & \cos \phi \\ \cos \theta & -\sin \theta & 0 \end{pmatrix} \begin{pmatrix} 0 \\ E_\theta^F \\ E_\phi^F \end{pmatrix} \quad (8)$$

Next, the Cartesian electric field of the feed is transformed from feed coordinate system to reflectarray reference system (R) by transformation matrix as described in 0 by:

$$\begin{pmatrix} E_x^R \\ E_y^R \\ E_z^R \end{pmatrix} = \mathbf{A} \begin{pmatrix} E_x^F \\ E_y^F \\ E_z^F \end{pmatrix} \quad (9)$$

and tangential electric field in the aperture is obtained as:

$$\vec{E}_{RC}(x, y) = E_x^R(x, y)\vec{x} + E_y^R(x, y)\vec{y} \quad (10)$$

where RC refers to Reflectarray Coordinate. The radiated electric field from the surface of the reflectarray antenna can be obtained from the equivalent magnetic current which is:

$$\begin{aligned} \vec{M} &= -2\hat{n} \times \vec{E}_{RC} = -2Z \times (E_x^R \vec{x} + E_y^R \vec{y}) \\ &= 2E_y^R \vec{x} - 2E_x^R \vec{y} \end{aligned} \quad (11)$$

Using equivalent magnetic current, vector potential F is obtained as described in [28] and far electric field radiated by the reflectarray antenna is expressed as:

$$\begin{aligned} \mathbf{E}(\theta, \phi) &= jk[(\hat{\theta} \cos \phi - \hat{\phi} \sin \phi \cos \theta) \tilde{E}_x^R(u, v) \\ &+ (\hat{\theta} \sin \phi - \hat{\phi} \cos \phi \cos \theta) \tilde{E}_y^R(u, v)] \frac{e^{-jk_0 r}}{2\pi r} \end{aligned} \quad (12)$$

where, $u = \sin \theta \cos \phi$, $v = \sin \theta \sin \phi$, and \tilde{E}_x^R and \tilde{E}_y^R are Fourier transforms of the Cartesian components E_x^R and E_y^R of the tangential electric field defined as:

$$\tilde{E}_{x/y}^R(u, v) = \iint_{RA} E_{x/y}^R(x, y) e^{jk_0(ux+vy)} dx dy \quad (13)$$

Considering that the reflected electric field in each element of the antenna has uniform amplitude and phase, we can write reflected electric field for each element as [22]:

$$E_{x/y}^{Rm,n}(md_x, nd_y) = E_{x/y}^{Rm,n} = A_{x/y}^{m,n} \exp(j\phi_{x/y}^{m,n}) \quad (14)$$

Slash in (14) means x or y components and $A_x^{m,n}$ and $\phi_x^{m,n}$ represent the amplitude and phase of the reflected field on the (m,n) element, and d_x and d_y are the element spacing. In order to evaluate the integral in (13) element by element, the following change of variables is defined for the coordinates (x, y) :

$$\begin{aligned} x &= x' + mP_x - \frac{(N_x-1)P_x}{2}; \quad m=0,1,2,\dots,N_x-1 \\ y &= y' + nP_y - \frac{(N_y-1)P_y}{2}; \quad n=0,1,2,\dots,N_y-1 \end{aligned} \quad (15)$$

In this equation central point of the element (m,n) is $(mP_x - \frac{(N_x-1)P_x}{2}, nP_y - \frac{(N_y-1)P_y}{2})$; and x' and y' are limited to a periodic cell $(-\frac{P_x}{2} \leq x' < \frac{P_x}{2}, -\frac{P_y}{2} \leq y' < \frac{P_y}{2})$.

N_x and N_y are the number of cells in the x and y direction. Therefore, (13) is calculated as:

$$\begin{aligned} \tilde{E}_{Rxi/y}(u, v) &= e^{-j\frac{k_0}{2}[u(N_x-1)d_x + v(N_y-1)d_y]} \\ &\sum_{m=0}^{N_x-1} \sum_{n=0}^{N_y-1} \left[e^{jk_0[ump_x + vnp_y]} \int_{-\frac{P_x}{2}}^{\frac{P_x}{2}} \int_{-\frac{P_y}{2}}^{\frac{P_y}{2}} E_{Rxi/y}^{m,n}(x', y') e^{jk_0[ux'+vy']} dx' dy' \right] \end{aligned} \quad (16)$$

So, after carrying out the integration on the periodic cells, \tilde{E}_x^R and \tilde{E}_y^R can be written as:

$$\tilde{E}_{x/y}^R(u, v) = S \sum_{m,n} A_{x/y}^{Rm,n} \exp[j\phi_{x/y}^{m,n} + jk_0(umd_x + und_y)] \quad (17)$$

where S is obtained from (16) as:

$$S = 4 \sin(0.5kud) \sin(0.5kvd) / kuv \quad (18)$$

Feed gain is related to its q factor. Electric field on each cell of the reflectarray antenna is obtained by (7) which is related to q factor of the feed. $A_x^{m,n}$ in (14) is the amplitude of the reflected field on the (m,n) element which is equal to the amplitude of $E_y^R(x, y)\vec{y}$ which is obtained from radiated electric field in the far field region of the feed antenna. Therefore, the effect of feed gain is considered in (7) up to (12). As a result, radiated far field for x polarized and y polarized feed can be written respectively as:

$$\vec{E}_x(u, v) = \frac{jk_0}{2\pi} S \left\{ \bar{w}_x \sum_{m,n} \Gamma_{x,x} E_x^{m,n} \exp[jk_0(umd_x + und_y)] + \bar{w}_y \sum_{m,n} \Gamma_{x,y} E_y^{m,n} \exp[jk_0(umd_x + und_y)] \right\} \quad (19)$$

$$\vec{E}_y(u, v) = \frac{jk_0}{2\pi} S \left\{ \bar{w}_y \sum_{m,n} \Gamma_{y,y} E_y^{m,n} \exp[jk_0(umd_x + und_y)] + \bar{w}_x \sum_{m,n} \Gamma_{y,x} E_x^{m,n} \exp[jk_0(umd_x + und_y)] \right\} \quad (20)$$

where $\bar{w}_x = (\hat{\theta} \cos \phi - \hat{\phi} \sin \phi \cos \theta)$, $\bar{w}_y = (\hat{\theta} \sin \phi - \hat{\phi} \cos \phi \cos \theta)$, $\Gamma_{x,x}$ is the reflection coefficient of x-polarization when unit cell is illuminated by x-polarized wave, $\Gamma_{x,y}$ is the reflection coefficient of x polarization when unit cell is illuminated by y-polarized wave, $\Gamma_{y,y}$ is the reflection coefficient of y polarization when unit cell is illuminated by y-polarized wave and $\Gamma_{y,x}$ is the reflection coefficient of y polarization when unit cell is illuminated by x-polarized wave. Moreover, transformation from (θ, ϕ) to co-polar (E_p) and cross-polar (E_q) components for an x-polarized feed horn, is given by:

$$\begin{pmatrix} E_p^x \\ E_q^x \end{pmatrix} = \begin{pmatrix} \cos \phi & -\sin \phi \\ -\sin \phi & -\cos \phi \end{pmatrix} \begin{pmatrix} E_\theta \\ E_\phi \end{pmatrix} \quad (21)$$

and, the transformation for a y-polarized feed horn is:

$$\begin{pmatrix} E_p^y \\ E_q^y \end{pmatrix} = \begin{pmatrix} \sin \phi & \cos \phi \\ \cos \phi & -\sin \phi \end{pmatrix} \begin{pmatrix} E_\theta \\ E_\phi \end{pmatrix} \quad (22)$$

Consequently, co-polar electric field in the far field region is calculated for x polarized and y polarized feed respectively by [22]:

$$|E_x| = \frac{k_0}{2\pi} |S| \left| 1 + \frac{(\sqrt{1-u^2-v^2}-1)u^2}{u^2+v^2} \right| \quad (23)$$

$$\sum_{m,n} A_x^{m,n} \exp[j\phi_x^{m,n} + jk_0(umd_x + vnd_y)]$$

$$|E_y| = \frac{k_0}{2\pi} |S| \left| \frac{(\sqrt{1-u^2-v^2}-1)uv}{u^2+v^2} \right| \quad (24)$$

$$\sum_{m,n} A_y^{m,n} \exp[j\phi_y^{m,n} + jk_0(umd_x + vnd_y)]$$

Also, cross polar electric field in the far field region is calculated for x polarized and y polarized feed respectively by:

$$|E_{cross-x}| = \frac{k_0}{2\pi} |S| \left| \frac{(\sqrt{1-u^2-v^2}-1)uv}{u^2+v^2} \right| \quad (25)$$

$$\sum_{m,n} A_x^{m,n} \exp[j\phi_x^{m,n} + jk_0(umd_x + vnd_y)]$$

$$|E_{cross-y}| = \frac{k_0}{2\pi} |S| \left| \frac{(\sqrt{1-u^2-v^2}-1)uv}{u^2+v^2} \right| \sum_{m,n} A_y^{m,n} \exp[j\phi_y^{m,n} + jk_0(umd_x + vnd_y)] \quad (26)$$

4-RESULTS

After obtaining required phase shift in each cell of the antenna, reflectarray antenna is designed using different cells and their gain is computed using (5) for the lower, center and upper frequency of the frequency band. Next, each designed antenna is analysed by full wave method to achieve co- and cross-polar levels of the antenna. As an example for gain of the antenna designed in the frequency band, gain of the antenna designed by double cross ring is shown in Fig. 5 at 11 GHz, 11.3 GHz, and 11.7 GHz. Also, in Fig. 6 to Fig. 12 the result of co- and cross-polarization levels obtained by simulation and full wave analysis for each designed antenna is shown. In these figures the results are obtained using equations (23) to (26) by written code in Matlab software and full wave analysis of the designed antennas is performed using FEKO software in which feed antenna is assumed as an external radiation pattern defined by (7).

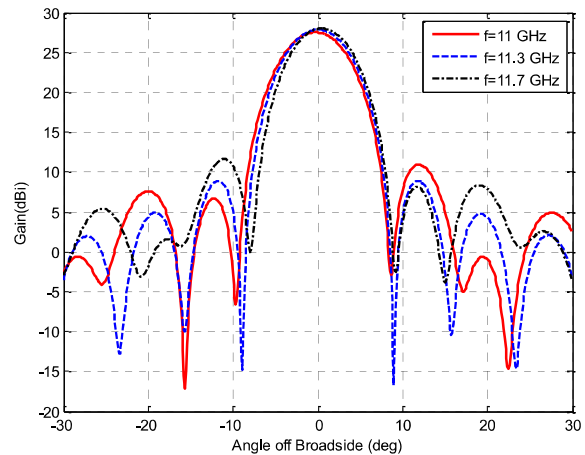


Fig. 5. Antenna gain designed by double cross ring

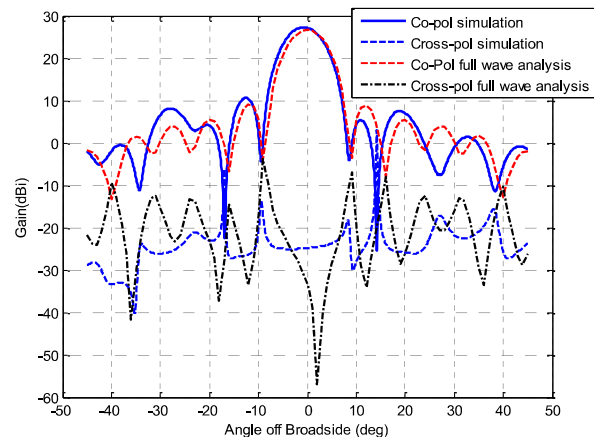


Fig. 6. Co-pol and cross-pol radiation pattern of the antenna in frequency of 11 GHz in full wave analysis for the antenna designed with rectangular patch cell

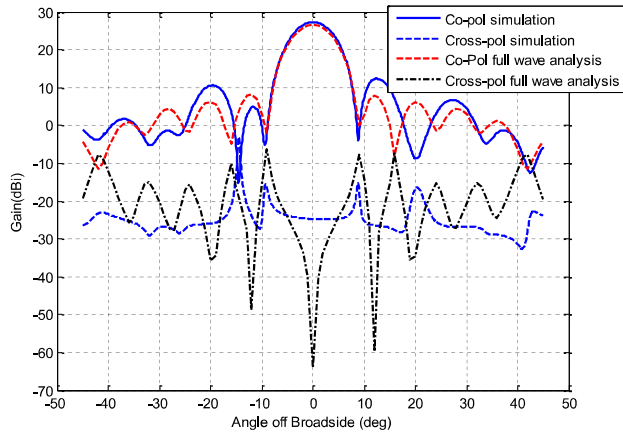


Fig. 7. Co-pol and cross-pol radiation pattern of the antenna in frequency of 11 GHz by full wave analysis for the antenna designed with double square cell

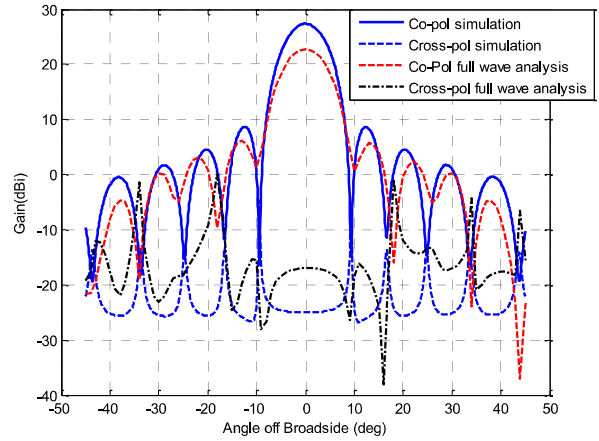


Fig. 10. Co-pol and cross-pol radiation pattern of the antenna in frequency of 11 GHz by full wave analysis for the antenna designed with circular patch with two stubs cell

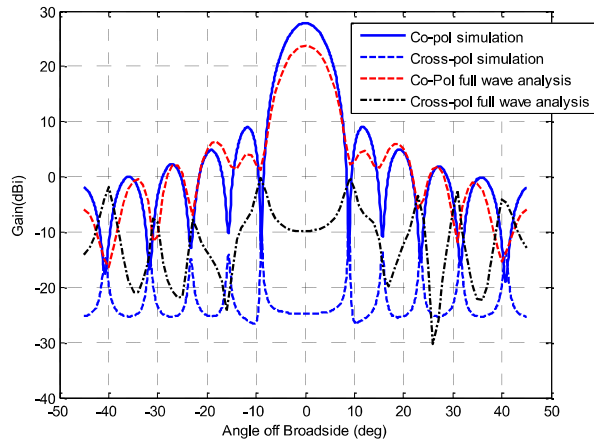


Fig. 8. Co-pol and cross-pol radiation pattern of the antenna in frequency of 11 GHz by full wave analysis for the antenna designed with circular patch with one stub cell

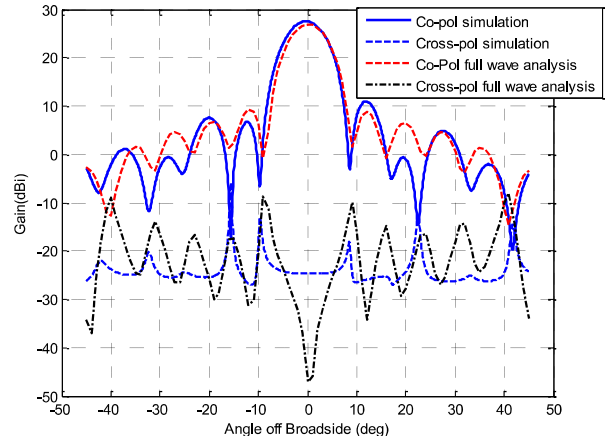


Fig. 11. Co-pol and cross-pol radiation pattern of the antenna in frequency of 11 GHz by full wave analysis for the antenna designed with double cross ring cell

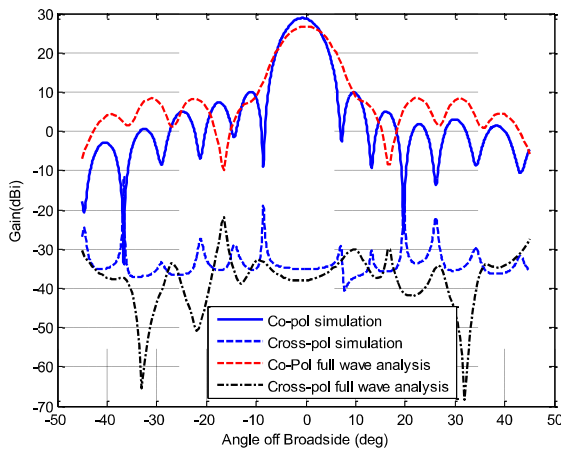


Fig. 9. Co-pol and cross-pol radiation pattern of the antenna in frequency of 11 GHz by full wave analysis for the antenna designed with three layer rectangle patch cell

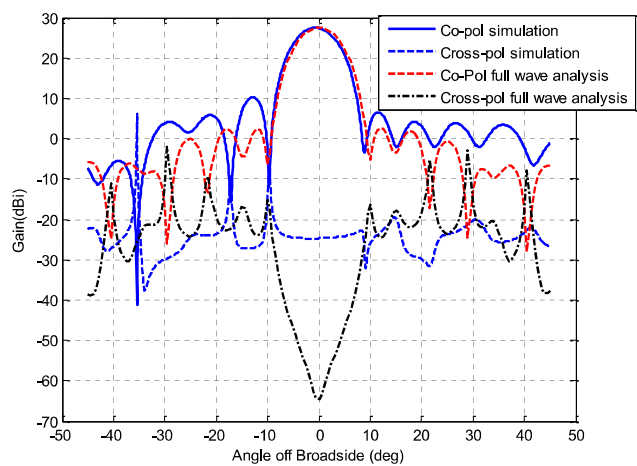


Fig. 12. Co-pol and cross-pol radiation pattern of the antenna in frequency of 11 GHz by full wave analysis for the antenna designed with rectangle cross ring cell

Moreover, in Fig. 13 cross polarization level of different designed antennas is compared against broadside angle which shows that circular patch with one stub has the worst result and rectangle and cross loop has the best cross-pol response.

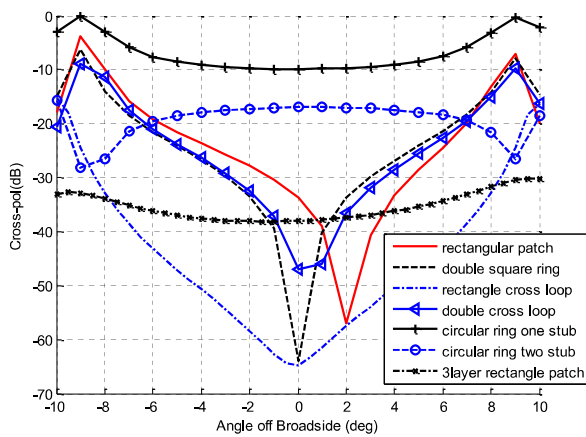


Fig. 13. Comparing cross-pol level of different designed antenna in frequency of 11 GHz by full wave analysis

Additionally, to see the results in the frequency band, gain and cross-pol level of different designed antennas in the frequency band of 10.5 GHz up to 12.5 GHz is compared in Fig. 14 and Fig. 15.

Designed antenna with double cross ring cell in this paper is compared with other published paper in Table 3.

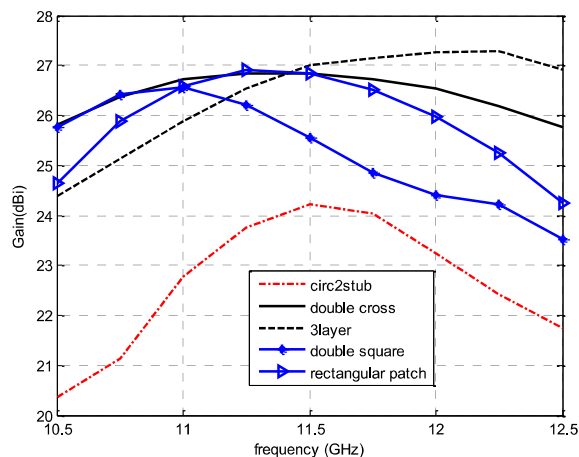


Fig. 14. Comparing gain of different designed antennas in the frequency band of 10.5 GHz up to 12.5 GHz by full wave analysis

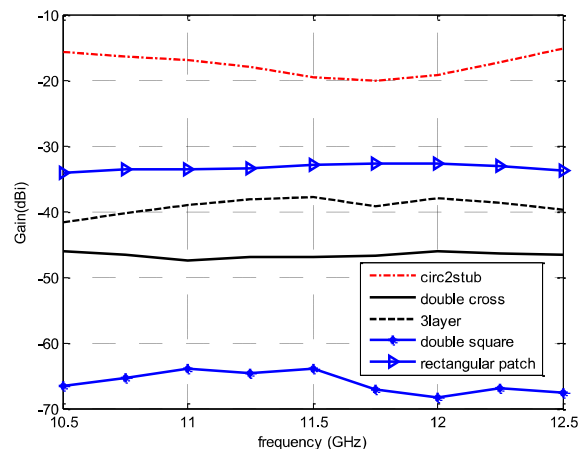


Fig. 15. Comparing cross-pol level of different designed antennas in the frequency band of 10.5 GHz up to 12.5 GHz by full wave analysis

TABLE 3. COMPARING THE RESULTS OF THIS PAPER WITH RESULTS OF OTHER PUBLISHED RESEARCH.

REF.	[21]	[23]	[24]	[26]	THIS WORK (DOUBLE CROSS)
SIZE (CM)	40×40	40×40	105×99	28×21	42×42
MAXIMUM GAIN (dBi)	33	31.6	not given	26.2	27
1 dB GAIN BANDWIDTH (%)	24	25	10	4	17
CENTRE FREQUENCY (GHz)	12.6	12	12	11.8	11
CROSS POL (dB)	-25	not given	not given	-38	-25
MAXIMUM CELL PHASE RANGE (DEGREES)	400	580	780	1000	610

5- CONCLUSION

We have proposed an efficient method to analyze reflectarray antennas. Our method utilizes the radiation properties of infinite arrays of specific types of unit cells which are obtained by applying periodic boundary conditions to a single unit cell. These elements are then used to design different high gain reflectarray antenna using phase synthesis. We also derived analytical expressions for obtaining co polar pattern of the antenna and calculating the cross polarization level. To confirm our derivations, we performed full wave simulations on the designed antennas. There was excellent agreement between our results and those obtained using full wave simulation. Full wave analysis of large reflectarray antenna is a computationally expensive task that is not feasible for very large antennas. Our method on the other hand can be used to efficiently and accurately model these antennas. Moreover, cross polarization level of different designed antennas against broadside angle is compared which shows that the antenna designed by circular patch with one stub cell has the worst

result and the antenna designed by rectangle and cross loop cell has the best cross-pol response.

ACKNOWLEDGEMENTS

The authors would like to thank Dr. Farhad Azadi Namin for his helpful comments.

REFERENCES

- [1] Pozar, D. M., and Metzler, T. A., "Analysis of a reflectarray antenna using microstrip patches of variable size", *Electron Lett* 29, pp 657–658, 1993.
- [2] Hamzavi-Zarghani, ; Z. Atlasbaf, "A new broadband single-layer dual-band reflectarray antenna in X- and Ku-Bands", *Antennas and Wireless Propagation Letters, IEEE Trans. Antennas Propagation*, pp 602 – 605, 2015.
- [3] Munson, R. E., Haddad, H. A., and Hanlen, J. W., "Microstrip reflectarray for satellite communications and RCS enhancement or reduction", U.S. patent 4 684 952, 1987.
- [4] Bialkowski, M. E., and Song, H. J., "Dual linearly polarized reflectarray using aperture coupled microstrip patches", *IEEE Int. Symp. Antennas Propagat*, pp 486–489, 2001.
- [5] B. D. Nguyen, K. T. Pham, V.-S. Tran, L. Mai, N. Yonemoto, A. Kohmura, et al., "Electronically tunable reflectarray element based on C-patch coupled to delay line," *Electronics Letters*, , pp 1114-1116, 2014.
- [6] Hasan Abadi, S.M.A.M. ; Ghaemi, K. ; Behdad, N. , "Ultra-wideband, true time delay reflectarray antennas using ground-plane-backed, miniaturized-element frequency selective surfaces", *IEEE Trans. Antennas Propagation* pp 534 – 542 , 2015.
- [7] T. Makdissy, R. Gillard, E. Fourn, E. Girard, and H. Legay, "Phase-Shifting Cell for Dual Linearly Polarized Reflectarrays with Reconfigurable Potentialities," 2013.
- [8] F. Venneri, S. Costanzo, and G. Di Massa, "Design and validation of a reconfigurable single varactor-tuned reflectarray," *Antennas and Propagation, IEEE Transactions on*, pp 635-645, 2013.
- [9] O. Bayraktar, O. A. Civi, and T. Akin, "Beam switching reflectarray monolithically integrated with RF MEMS switches," *Antennas and Propagation, IEEE Transactions on*, pp 854-862, 2012.
- [10] M. Riel and J. Laurin, "Design of an electronically beam scanning reflectarray using aperture-coupled elements," *Antennas and Propagation, IEEE Transactions on*, pp 1260-1266, 2007.
- [11] F. Venneri, S. Costanzo, and G. Di Massa, "Reconfigurable aperture-coupled reflectarray element tuned by single varactor diode," *Electronics Letters*, 68-69, 2012.
- [12] B. D. Nguyen, K. T. Pham, V.-S. Tran, L. Mai, N. Yonemoto, A. Kohmura, et al., "Electronically tunable reflectarray element based on C-patch coupled to delay line," *Electronics Letters*, pp 1114-1116, 2014.
- [13] S. Montori, F. Cacciamani, R. Vincenti Gatti, R. Sorrentino, G. Arista, C. Tienda Herrero, et al., "A Transportable Reflectarray Antenna for Satellite Ku-band Emergency Communications."
- [14] E. Carrasco, M. Barba, and J. A. Encinar, "X-band reflectarray antenna with switching-beam using pin diodes and gathered elements," *Antennas and Propagation, IEEE Transactions on*, pp 5700-5708, 2012.
- [15] A. E. Martynyuk, J. Martinez Lopez, and N. A. Martynyuk, "Spiraphase-type reflectarrays based on loaded ring slot resonators," *Antennas and Propagation, IEEE Transactions on*, pp 142-153, 2004.
- [16] H. Kamoda, T. Iwasaki, J. Tsumochi, T. Kuki, and O. Hashimoto, "60-GHz electronically reconfigurable large reflectarray using single-bit phase shifters," *Antennas and Propagation, IEEE Transactions on*, pp 2524-2531, 2011.
- [17] E. Carrasco, J. A. Encinar, and M. Barba, "Dual linear polarized reflectarray element with true-time delay," in *Antennas and Propagation, 2009. EuCAP 2009. 3rd European Conference on*, 2009, pp. 3733-3737.
- [18] R. Pereira, R. Gillard, R. Sauleau, P. Potier, T. Dousset, and X. Delestre, "Four-state dual polarisation unit-cells for reflectarray applications," *Electronics letters*, pp 742-743, 2010.
- [19] G. Perez-Palomino, R. Florencio, J. A. Encinar, M. Barba, R. Dickie, R. Cahill, et al., "Accurate and Efficient Modeling to Calculate the Voltage Dependence of Liquid Crystal Based Reflectarray Cells", *IEEE Trans. Antennas Propagation*, pp 2659 – 2668, 2014.
- [20] Bialkowski, M. E., and Sayidmarie, K. H., "Investigations into phase characteristics of a single-layer reflectarray employing patch or ring elements of variable size", *IEEE Trans. Antennas Propagation* 56, 2008.
- [21] Chaharmir, M. R., and, J. Shaker, "Broadband reflectarray with combination of cross and rectangle loop elements", *Electron Let* 44, 658–659, 2008.
- [22] Huang, J., and Encinar, J. A., *Reflectarray*

-
- Antennas, IEEE Press. New York, John Wiley & Sons, 2008.
- [23] Chaharmir, M. R., Shaker J., and Legay, H., “Broadband design of a single layer large reflectarray using multi cross loop elements”, IEEE Trans. Antennas Propagation 57, pp 3363-3366. 2009.
- [24] Encinar, J. A., and Zornoza, J. A., “Broadband design of three-layer printed reflectarrays”, IEEE Trans. Antennas Propagation 51, pp 1662–1664, 2003.
- [25] Hasani, H., Kamyab, M., Mirkamali, A., “Low cross polarization reflectarray antenna”, IEEE Trans. Antennas Propagation 59, pp 1752 – 1756. 2011.
- [26] Malfajani, R. S., Atlasbaf, Z., “Design and implementation of a broadband single layer reflectarray antenna with large range linear phase elements”, IEEE Antennas and Wireless Propagation Letters 11, pp 1442–1445, 2012.
- [27] Rahmat-Samii, Y., “Useful coordinate transformations for antenna applications”, IEEE Trans. Antennas Propagation, pp 571 – 574. 1979.
- [28] Balanis, C. A., “Advanced engineering electromagnetic”, IEEE Press, John Wiley & Sons New York, 2012.